DETECTION OF FRACTURES IN PRESTRESSING STEEL STRANDS USING THE MAGNETIC FLUX LEAKAGE TEST CONSIDERING A VARIETY OF PHYSICAL AND GEOMETRIC PARAMETERS

DETEKTION VON SPANNSTAHLBRÜCHEN MIT DER MAGNETISCHEN STREUFELDMESSUNG UNTER VARIATION PHYSIKALISCHER UND GEOMETRISCHER PARAMETER

Jonathan Villing, Frank Lehmann, Michael Schreiner

Materials Testing Institute (MPA), University of Stuttgart, Otto-Graf-Institute

SUMMARY

The magnetic flux leakage test has been in use at the Materials Testing Institute at the University of Stuttgart for several decades. The detection of fractures in prestressing steel strands with this method is subject to a large number of physical and geometric parameters. These parameters were varied in laboratory tests and analysed by statistical methods, whereby the elementary influencing factors could be separated. In addition, the influence of regular and irregular magnetic interferences was quantified.

ZUSAMMENFASSUNG

Die magnetische Streufeldmessanlage ist seit mehreren Jahrzehnten an der Materialprüfungsanstalt Universität Stuttgart im Einsatz. Die Detektion von Spannstahlbrüchen mit diesem Verfahren unterliegt einer Vielzahl physikalischer und geometrischer Parameter. Diese Parameter wurden in Laborversuchen variiert und durch statistische Methoden analysiert, wodurch die elementaren Einflussfaktoren separiert werden konnten. Außerdem wurde der Einfluss regelmäßiger und unregelmäßiger magnetischer Störeinflüsse quantifiziert.

1. INTRODUCTION

The institute has been invited for a proficiency test on prefabricated girders by DB Systemtechnik GmbH and MFPA Leipzig. This opportunity was used to evaluate the detection of fractures in prestressing steel strands, taking into account a variety of physical and geometric parameters. For this purpose, the specimen from the proficiency test was simulated in the laboratory and a large number of different fractures in steel strands were installed and tested under varying boundary conditions. The goal of these tests and the subsequent evaluation was to analyse the influencing factors on the detection of fractures.

The detection of fractures with the magnetic flux leakage test is fundamentally susceptible to magnetic interference, which is reduced by the multi-stage filter methods. Rebars with different spatial orientations and diameters were examined for the systematic investigation of irregular interference sources in the test area.

2. THEORETICAL BACKGROUND

The magnetic flux leakage test is designed to consider typical construction methods with a combination of rebars and prestressing steel, it relies heavily on the differing magnetic properties of these components. Therefore, it is useful to have a basic understanding of the physical processes to interpret the measurement data.

2.1 Magnetic material properties

One of the most decisive physical prerequisites for the method is the magnetic material behaviour of reinforcing steel and prestressing steel. Both materials have a ferromagnetic behaviour, whereby reinforcement is soft-magnetic and prestressing steel is hard-magnetic [1].

Ferromagnetic materials have atomic magnetic moments that are naturally rectified within magnetic domains. This is illustrated in Fig. 1. In this illustration, each arrow represents an atomic magnetic moment and within each boundary line is a magnetic domain. The boundary lines represent the domain walls, which subdivide into Bloch walls and Néel walls depending on the rotation of the magnetisation [2, 3].

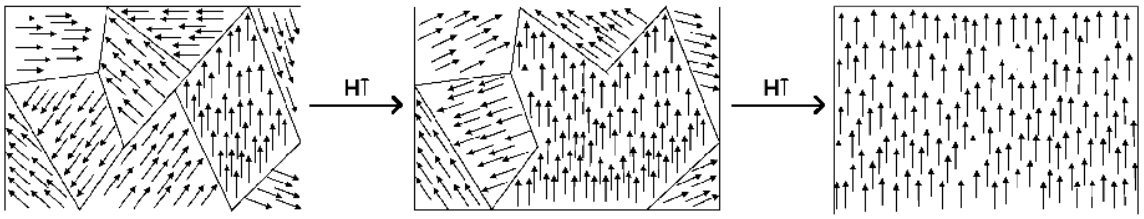

Fig. 1: Illustration of magnetic domains [11]

The natural state without an external magnetic field is shown in Fig. 1 on the left. The magnetic moments of the atoms are parallel within the magnetic domains. However, since the domains point in different directions, the ferromagnetic material as a whole is not magnetic. When an external magnetic field is applied to the material, the domains align more and more in the direction of the field (Fig. 1, centre) until complete alignment in the direction of the magnetic field is achieved (Fig. 1, right). While the magnetic domains align, the Bloch walls are usually abruptly shifted or, in rare cases, the magnetic moments of a domain are aligned in the field direction by flipping spontaneously. Part of this complex process is explained by the Barkhausen effect. This magnetic order can be reversed by external shocks or by heating beyond the Curie temperature. The Curie temperature for iron is 768 °C [2, 3].

In addition to vibrations and an increase in temperature, the magnetisation can also be manipulated and cancelled out by an opposing magnetic field. However, this relationship is not linear, it follows a hysteresis curve. Fig. 2 shows the hysteresis curves of reinforcing steel and prestressing steel of the type Sigma oval. The new curve is not included in this illustration. It starts at $H_0 = 0$ A/cm and $M_0 = 0$ A/cm when the external magnetic field is passive. As the field strength H of the external magnetic field is increased M asymptotically approaches the saturation value. The magnetisation of the ferromagnetic material cannot be increased beyond the saturation. If the external magnetic field is removed, which in practice corresponds to switching off the electromagnet, the magnetisation does not return to $H_0 = 0$ A/cm. Instead, a magnetisation remains, which is called remanence. The remanence is also the intersection of the magnetisation curve with the y-axis. To cancel out the magnetisation of the ferromagnetic material, you have to apply an oppositely directed magnetic field. This can be done by reversing the polarity of an electromagnet or by moving the same magnetic field in the opposite direction. The field strength required for the magnetisation to be M = 0 A/cm is called the

coercive magnetic field strength and is the point of intersection of the magnetisation curve with the x-axis [2, 3].

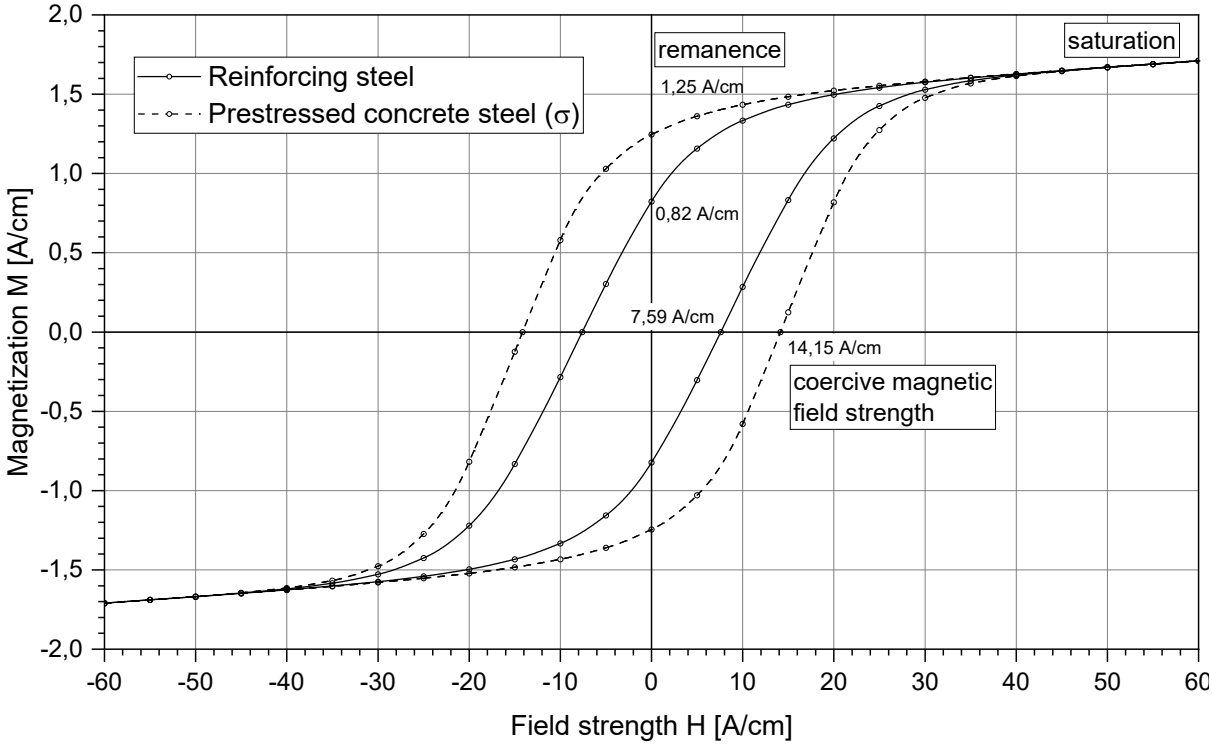

Fig. 2: Hysteresis curve of reinforcing steel and prestressing steel (Sigma oval)

These properties of ferromagnetic materials are used in different ways in magnetic flux leakage testing. A crucial point is, that only three elements have ferromagnetic properties at room temperature: iron, nickel and cobalt. Apart from these, there are only a few alloys, such as permalloy or mumetal, that have such properties. However, these materials are rare and expensive, which is why they are not used in the construction sector. Apart from the types of steel typically used in construction, there are usually few magnetic interferences to be found in buildings. In particular, the concrete that encases the steels does not interfere with the magnetic flux leakage test. Furthermore, the ferromagnetic properties of different types of steel differ. Fig. 2 shows the hysteresis curves of reinforcing steel and prestressing steel of the type Sigma oval. It can be seen that the curves have a different shape and the remanence and coercive magnetic field strengths differ from each other. Prestressing steel has a remanence of $M_R = 1.25$ A/cm and reinforcing steel of $M_R = 0.82$ A/cm. The coercivity of prestressing steel is $H_C = 14.15$ A/cm and of reinforcing steel $H_C = 7.59$ A/cm. In this context, reinforcing steel is referred to as soft magnetic and prestressing steel as hard magnetic.

These properties are used in the filtering of the magnetic signals, which is described in the next chapter. By looking carefully at the curves, one can already make some basic considerations: If the steels are first magnetised to saturation and the magnet is then switched off, remanence will occur in both steels. The magnetisation of the prestressing steel will be higher than that of the reinforcing steel. At this point, if the magnetic field strength is reversed and the coercive magnetic field strength of the reinforcing steel is applied, the magnetisation of the reinforcing steel becomes M = 0 A/cm. Meanwhile, a residual signal from the prestressing steel is maintained [1-4].

2.2 Magnetic flux leakage test

Magnetic flux leakage testing is a non-destructive method used to detect fractures in prestressing steel. The components to be tested are magnetised with the help of an external magnetic field, which causes them to form a magnetic stray field themselves. If the magnetised prestressing steel has a fracture, a magnetic dipole forms, which locally changes the magnetic stray field. If the stray field along the prestressing steel strands are measured with magnetic field sensors, this anomaly can be detected. The data is evaluated in the form of magnetisation curves. The fracture induces a local maximum and has a specific shape that can be filtered out in a multi-stage filtering process. The specific shape is illustrated in Fig. 3 [5-7].

The ferromagnetic properties of the steel are used to analyse the magnetic fields. The magnetic stray fields are measured during several measurement runs, both during the magnetisation process and with the magnet switched off. A stray field measurement is obtained in the active field and a remaining field measurement in the passive field. This process is outlined in Fig. 3 [5].

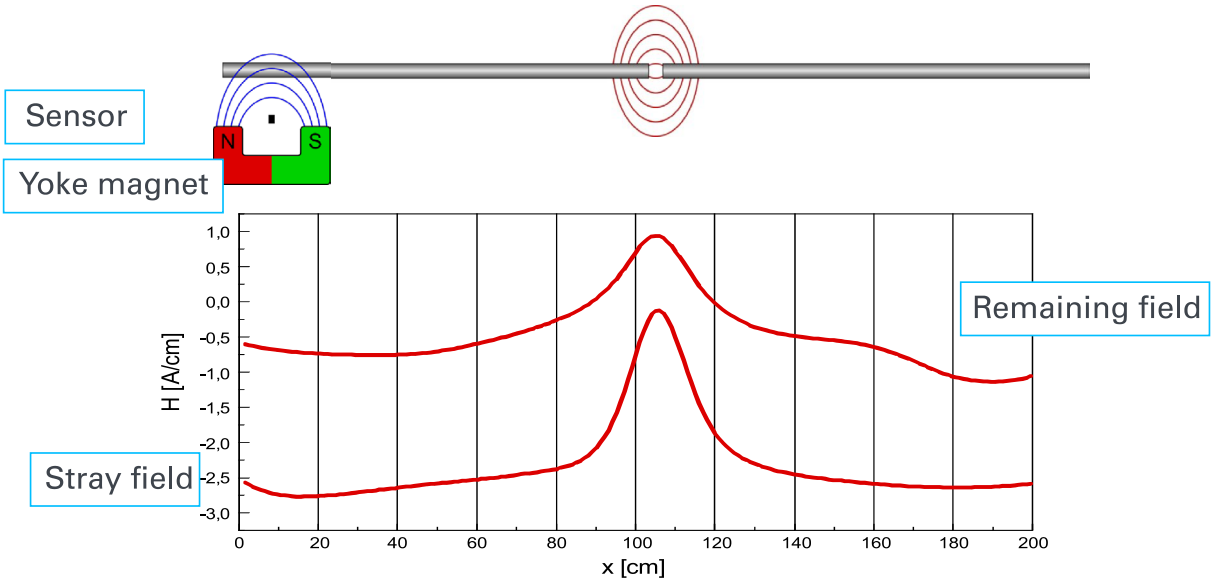

Fig. 3: Sketch of the process for measuring the magnetic field

In real structures that are inspected with magnetic flux leakage test, reinforcement is also installed in addition to the prestressing steel. In the measurement process described above, it is not only the prestressing steel that is measured. The reinforcement is also magnetised and forms magnetic stray fields. Especially stirrups form specific magnetic fields that make the detection of fractures more difficult. For this reason, different methods have been developed to suppress the influence of the stirrups as much as possible. First, the components to be examined are tested in several successive magnetisation runs. Measurements are taken on each outward journey, regardless of whether the magnet is active or passive. A typical sequence of measurement runs is shown in Table 1. The measurement runs 1 to 4 are used for magnetisation and gradual demagnetisation with detection of the stray field. In measurement run 5, the remaining field measurement 1 is carried out on the outward run and the magnetisation of the stirrups is reversed on the return run. Measurement run 6 records the remaining field 2 after reversal of the magnetisation. The aim of this sequence is to achieve the most uniform magnetisation of the prestressing steel with the lowest possible magnetisation of the reinforcing steel [1, 5].

Table 1: Typical measurement runs for recording stray fields and remaining fields

No.	I_{out} [A]	I_{return} [A]	Function
1	8	0	Magnetisation and gradual demagnetisation with detection of the stray field
2	6	0	
3	4	0	
4	2	0	
5	0	2	Remaining field measurement 1 and reversal of the magnetisation of the stirrups
6	0	0	Remaining field measurement 2 after reversal of the magnetisation

In order to filter the interferences of the reinforcing steel, the two remaining field measurements are added. By reversing the stirrup magnetisation, the signals cancel each other out, while the magnetisation of the tendon in the longitudinal direction is preserved. For further filtering of the signals, locations of the stirrups are calculated and then smoothed. For this purpose, the remaining field signals are differentiated in x-direction and the x-component of the local maxima are calculated. Subsequently, idealised stirrup signals are fitted to the measured stirrup signals using the best-fit method and variable weighting coefficients. Since the superposition principle applies to the remaining field measurements, the signals of the stirrups can be suppressed [5].

The last evaluation step is a correlation analysis of the filtered remaining field measurements with an idealised fracture signal. The fracture signal was determined analytically and verified by laboratory measurements. From this, the correlation coefficient $r(x)$ is obtained, which is then multiplied by the pole strength $P(x_0)$. With the expression $r(x) \cdot P(x_0)$ the fracture amplitude is calculated. The greater the fracture amplitude, the more likely a fracture in prestressing steel is at the corresponding point [5].

The strength of the fracture amplitude is determined by the following influencing factors:

- Probe distance
- Reinforcement
- Fracture of the prestressing steel
    - Fracture width
    - Cross-sectional reduction
    - Fracture orientation.

The distance of the probe is one of the most important influencing factors for the evaluation of fracture amplitudes. In theory, the signal amplitudes decrease proportionally to z^{-2}. This could also be demonstrated in laboratory experiments by Walther [5, 8].

The influence of reinforcement is difficult to quantify because individual reinforcement arrangements are decisive. It differs from the other influencing factors as it has no direct systematic influence on the fracture amplitude. Reinforcing steel can influence the signals of prestressing steel fractures in many ways. Among them are shielding and superposition effects that can attenuate or even suppress fracture amplitudes. In the case of strong cross-sectional reductions of the prestressing steel with high fracture amplitudes, the fractures remain reliably detectable. However, in the case of smaller or geometrically complex cross-sectional reductions with low fracture amplitudes, the influence of the reinforcement becomes more and more important. Specific reinforcement arrangements and other magnetic influences can also cause fracture-like signals. Typical arrangements of that kind include lap joints of longitudinal or mesh reinforcement and free ends of rebars [1, 4, 5].

The fracture width is by definition the distance between the fracture edges. In a real-life situation, however, this distance is difficult to determine because the fracture edges have uneven geometries. In addition, the fracture width depends, among other things, on the ungrouted areas within the cladding tube, the frictional forces between the prestressing steel and the bond between the prestressing steel and the grout. In practice, fracture widths of 1 to 2 mm normally occur in well grouted conditions. Under less favourable conditions, however, the fracture edges

may be further apart. The influence of the fracture width on the fracture amplitudes is well documented. For very small fracture widths up to 1 mm, the influence of the fracture width is relatively large. If the fracture width is then increased further, it approaches a limit value. Already at 0.5 mm, 80 % of the maximum fracture amplitude is reached. The maximum of the fracture amplitude is reached at about 3 mm [4, 9].

Cross-sectional reduction is only decisive for bundles of prestressing steel. For single strands and complete fractures, the test is relatively reliable. Cracks in prestressing rods or single strands can generally not be detected. Therefore, cross-sectional reduction can only occur in this case if whole bars are broken. A common theory to explain the behaviour of bundles in which only part of the strands are broken is that the magnetic flux emerging from the fracture induces an additional magnetisation in the intact steels, whose stray field is opposite to the original stray field of the fracture. This leads to a reduction in the measured magnetisation and thus in the fracture amplitudes. The influence of cross-sectional reduction is usually mentioned indirectly in the literature as an application limit. A cross-sectional reduction of 20 % or more is usually stated as reliably detectable. It has already been stated in the scientific literature that the influence of cross-sectional reduction on the fracture amplitude is almost proportional [1, 4, 5, 8, 9 10].

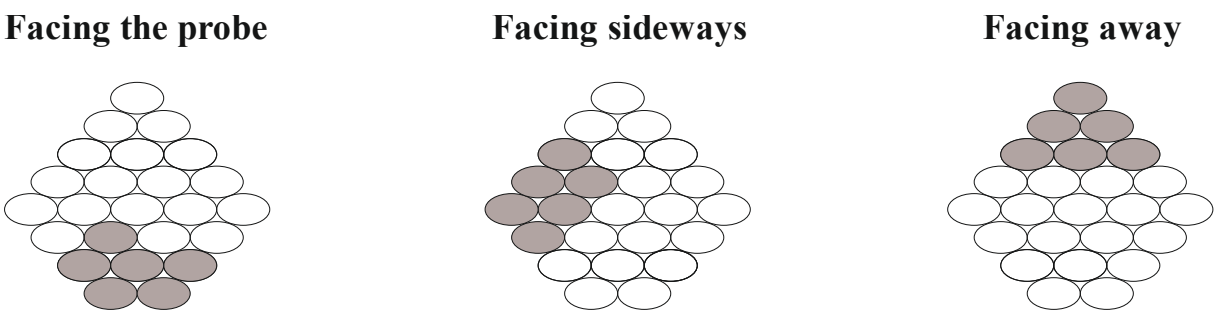

Fig. 4: Fracture orientations related to the probe from below

The influence of the fracture orientation was dealt with extensively in the diploma thesis of Steinfeld [4]. He positioned the fracture edges of different cross-sectional reductions and bundle sizes facing the probe and facing away from it. Fig. 4 illustrates these orientations for a cross sectional reduction of 25 % when 6 of 24 strands are broken. For example, he conducted two series of tests on a bundle of 35 steels of the type Sigma oval. When testing the fractures, the fracture was first rotated facing the probe and then was turned facing away. The comparison of the two fracture orientations shows a reduction in fracture amplitudes between

64 % and 84 % with cross-sectional reductions between 5.71 % and 45.71 %. Considering all of his results Steinfeld concluded that the influence of the fracture orientation is so decisive that a statement about the cross-sectional reduction is not possible without knowledge of the fracture orientation [4].

3. EXPERIMENTAL SETUP

To carry out the magnetic flux leakage test, a probe and magnet is moved on a measuring rail under the test object. Probe and magnet are moved evenly on the measuring rail with the help of a stepper motor at speeds between 10 and 30 cm/s. All tests were carried out with a measuring speed of 30 cm/s. Fig. 5 shows an overview of the experimental setup. The reinforcement cage was made of reinforcing steel of the type B500B. It had a length of 6 metres, a width of 0.5 metres and a height of 0.8 metres. The longitudinal rebars had a nominal diameter of d = 12 mm and the stirrups had two different diameters: d = 16 mm and d = 8 mm.

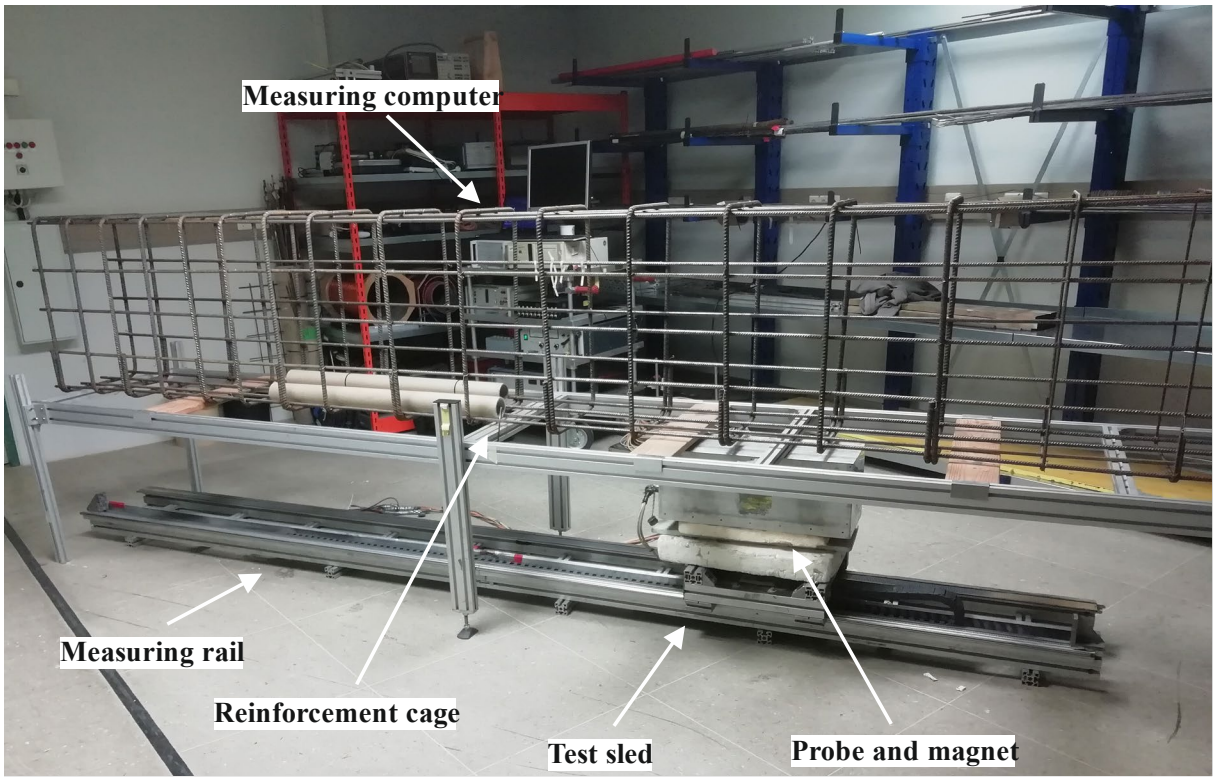

Fig. 5: Overview experimental setup

In this setup two layers of two prestressing steel strands each were installed. The lower layer was made of the type Sigma oval (St 145/160). The distance from the probe was varied between 6.4 and 10.5 cm. The upper layer was made of the type

Neptun oval (St 145/160). The distance from the probe was constant at 26.4 cm, but in some test series it was removed to see the effects. Each strand consisted of 24 single wires. In one of the lower strands up to 25 % of the cross-sectional area were installed as fractured. The fracture width was a constant 1 mm in each test.

4. EXPERIMENTAL PROCEDURE

Various tests were carried out in the basic test setup. In the following two chapters, the experimental procedures for quantifying the influencing factors of fracture detection and magnetic interference are presented. Both procedures were performed with the protocol shown in Table 12.

4.1 Fracture detection

With the aim of investigating as many different influencing factors as possible, nine test series were designed. Up to six strands with complete fractures were installed. This resulted in six different cross-sectional reductions in each test series: 4 %, 8 %, 13 %, 17 %, 21 % and 25 %. For each cross-sectional reduction, three different fracture orientations and two different positions in relation to stirrups were tested. Multiplying these variations gives 36 measurements that made up each test series. The three different fracture orientations are illustrated in Fig. 4. The two different positions in relation to stirrups are shown in Fig. 6. The stirrups were expected to magnetically shield the fracture, which should have reduced the fracture amplitude.

Those 36 variations of the parameters were repeated in each of the nine test series. For each of these test series, different boundary conditions applied, which are summed up in Table 2. Open stirrup ends occur when the stirrups are bent. The ends of the stirrups overlap, so at this point the double amount of reinforcing steel in combination with the open ends of the stirrups could have a magnetic effect. To see if this reinforcement arrangement has an influence on the test results, the reinforcement cage was turned around after test series 4. When the open ends of the stirrups face away they are out of reach of the probe. After the reinforcement cage was turned around and the open ends were facing the probe, they were even closer to the probe than the prestressing steel.

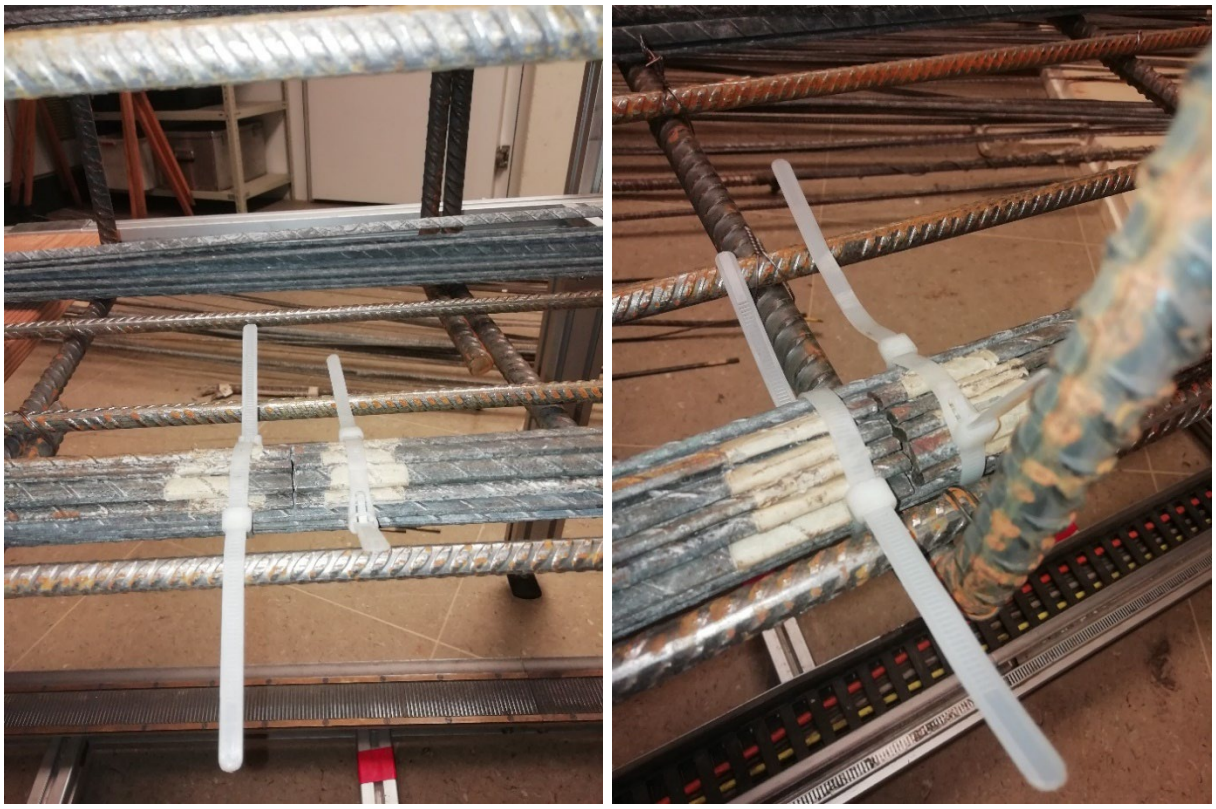

Fig. 6: Examples of the fracture width and position in relation to stirrups (left: in between stirrups, right: over stirrup)

Table 2: Overview of the test series 1 to 9

No.	Distance of the probe	Upper layer installed?	Stirrup diameter	Open ends of the stirrups
Test series 1	6.3 cm	No	16 mm	Facing away
Test series 2	6.3 cm	No	16 mm	Facing away
Test series 3	6.3 cm	Yes	16 mm	Facing away
Test series 4	10.5 cm	Yes	16 mm	Facing away
Test series 5	6.3 cm	Yes	16 mm	Facing the probe
Test series 6	10.5 cm	Yes	16 mm	Facing the probe
Test series 7	10.5 cm	Yes	8 mm	Facing the probe
Test series 8	6.3 cm	Yes	8 mm	Facing the probe
Test series 9	6.3 cm	Yes	8 mm	Facing the probe

4.2 Magnetic interferences

The reinforcement cage is a form of regular magnetic interference in which the spacing of the stirrups is regularly repeated along the measurement path. This type of arrangement has long been treated with the invention of the multi-stage filter method. In reality, reinforcement arrangements are often irregular and not perfectly documented in the plans. To investigate the influence of irregular magnetic interferences, single rebars with open ends were installed.

Each orientation was installed with bar diameters of 8 mm, 12 mm and 20 mm reinforcing steel B500B. The bars used had lengths between 60 cm and 75 cm. These rebars were installed in six different spacial orientations, which are shown in Table 3. These orientations were first tested separately without interference, then they were inserted into the reinforcement cage, after which unbroken prestressing steel strands were added and finally a fracture was installed next to the additional rebar.

Table 3: Investigated orientations of the rebars

Rotation x-z	**Rotation x-y**
90°	0°
45°	0°
45°	45°
45°	90°
45°	135°
45°	180°

Two examples of those arrangements are shown in Fig. 7. The probe distance to the prestressing steel was 4 cm. The lower open ends of the rebars were thus only 2.4 cm away from the probe, which should have a stronger influence than in most cases of practice. Subsequently, a cross-sectional reduction of 25 % was applied directly next to the additional rebar. It was first tested without the additional rebar and then with all the different diameters and orientations to determine the effect on the fracture amplitudes. This was investigated considering two fracture orientations and positions in relation to stirrups.

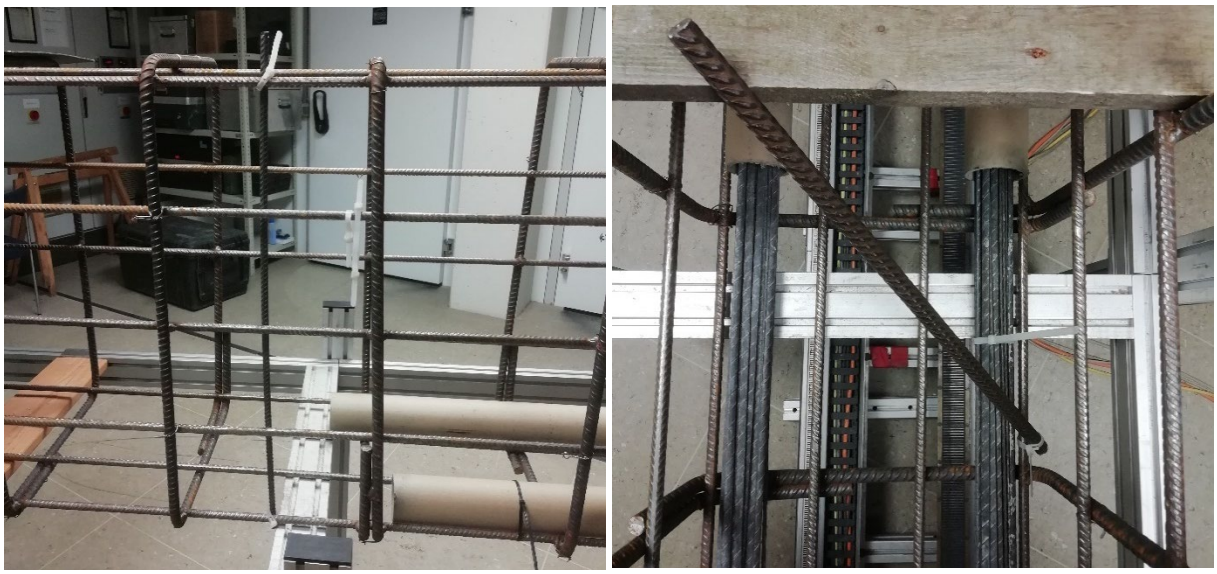

Fig. 7: Exemplary arrangement of rebars in the reinforcement cage to assess the magnetic interference Left: without prestressing steel Right: with without prestressing steel

5. RESULTS AND DISCUSSION

A total of 408 different set-ups were tested for fracture detection and another 181 for magnetic interferences. In this chapter, only the most informative results are discussed.

5.1 Fracture detection

In every set-up all of the influencing factors were present. By re-sorting, filtering, graphical and statistical methods, the influencing factors could be separated and evaluated. The following modalities were assessed first:

- Fracture orientation
- Cross-sectional reduction
- Position in relation to stirrups
- Probe distance.

Subsequently, the following subcategories were formed:

- Fracture orientation and cross-sectional reduction
- Position in relation to stirrups and cross-sectional reduction
- Probe distance and cross-sectional reduction.

For the following categories, the sample size was partly too small to make a clear statistical statement. However, one can compare the results with the statistically more relevant categories to verify them:

- Probe distance and fracture orientation
- Probe distance, fracture orientation and only 25% cross-sectional reduction
- Cross-sectional reduction, fracture orientation and only 6.3 cm probe distance
- Cross-sectional reduction, fracture orientation and only 10.5 cm probe distance.

In order to evaluate the categories, the detection probability and the fracture amplitude were in the foreground. As a first evaluation step, it was assessed how many of the installed fractures were found. For the analysis of the fracture amplitudes, only found fractures were included. Within a group, the mean and median of the fracture amplitudes were calculated. In order to compare the groups with each other, the fracture amplitude reduction related to the mean value was chosen.

In the literature, a cross-sectional reduction of at least 20 % is specified as the process limit in order to reliably detect a fracture. The experimental procedure included a large number of fractures whose detection was not expected from the outset.

5.1.1 Fracture orientation

The probability of detection is reliably highest for fractures facing the probe. If all values are included, it is 75 %. Fractures facing sideways can be detected with a probability of 48 % and fractures facing away with 40 %. This order of magnitude is also confirmed by the subcategories. It is surprising that the difference between fractures facing sideways and facing away is so little, especially when one considers the big difference between facing and facing away.

If no further subcategories are formed, but all values are included, then the break amplitude is reduced from "facing" to "facing sideways" by 49 % and to "facing away" by 58 %. This order of magnitude is confirmed for cross-sectional reductions between 13 % and 25 %, where the mean value of the reduction from "facing" to "facing sideways" is 45 % and to "facing away" 60 %. If cross-sectional reductions of less than 10 % are included the amplitude reductions are lower. This

may be related to the smaller sample sizes at smaller cross-sectional reductions, as fewer fractures were found. With a probe distance of 10.5 cm and a division according to cross-sectional reduction, this clear behaviour cannot be recognised. The mean value of the fracture amplitude reduction from "facing" to "facing sideways" is 22 % and to "facing away" 26 %. The lower reduction can be explained by the fact that the fracture amplitudes are generally lower with a larger probe distance. The larger scatter of the reductions at different cross-sectional reductions may also be due to the smaller sample sizes in this evaluation modality.

In summary, the fracture amplitude reduction from "facing" to "facing sideways" is 47 % and to "facing away" 62 %. This is true for a cross-sectional reduction of more than 10 % and a constant probe spacing. The influence of the probe distance seems to be more complex than the cross-sectional reduction, which is discussed in detail in the influence factor probe spacing.

5.1.2 Cross-sectional reduction

The degree of cross-sectional reduction is reliably related to the probability of detection. Fig. 8 shows this with an almost linear increase. By and large, this is also confirmed when further subcategories are included. For example Fig. 9 shows the detection probability considering the cross-sectional reduction and the fracture orientation. Particularly important for the established application limits is the detection probability for cross-sectional reduction above 20 %. Including all data, the probability at 21 % cross-sectional reduction is 85 % and at 25 % cross-sectional reduction it is 93 %. This order of magnitude is also confirmed in the other subcategories. A deviation from this is an increase in the probe distance. At a cross-sectional reduction of 25 % and a probe distance of 4 cm, 100 % of the fractures are detected, at 6.3 cm it is also 100 % and at 10.5 cm it is 62 %. The fracture amplitude reduction behaves similarly to the detection probability. This almost linear behaviour is illustrated in Fig. 10. There are small deviations in the subcategories. However, the general behaviour indicates a linear relationship between cross-sectional reduction and fracture amplitude reduction. This is consistent with the results from comparable research projects.

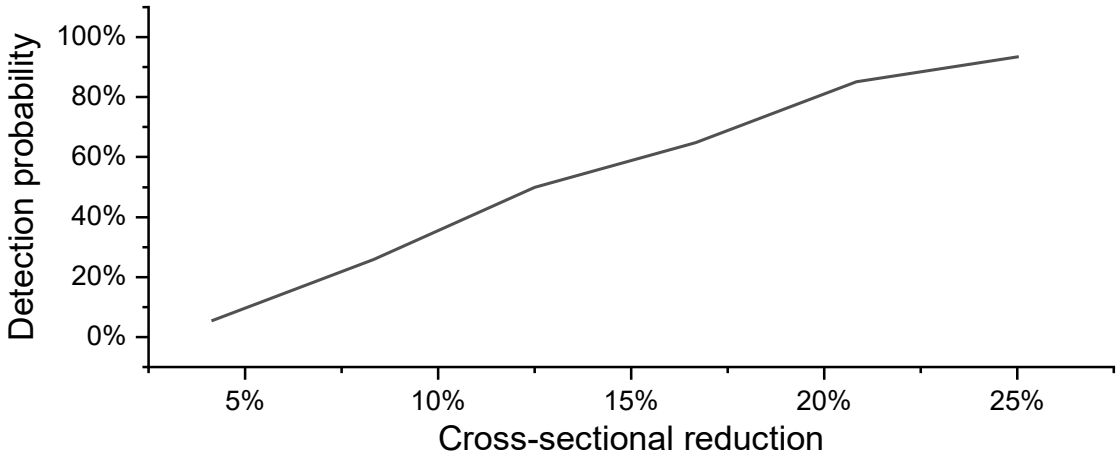

Fig. 8: Detection probability considering cross-sectional reduction

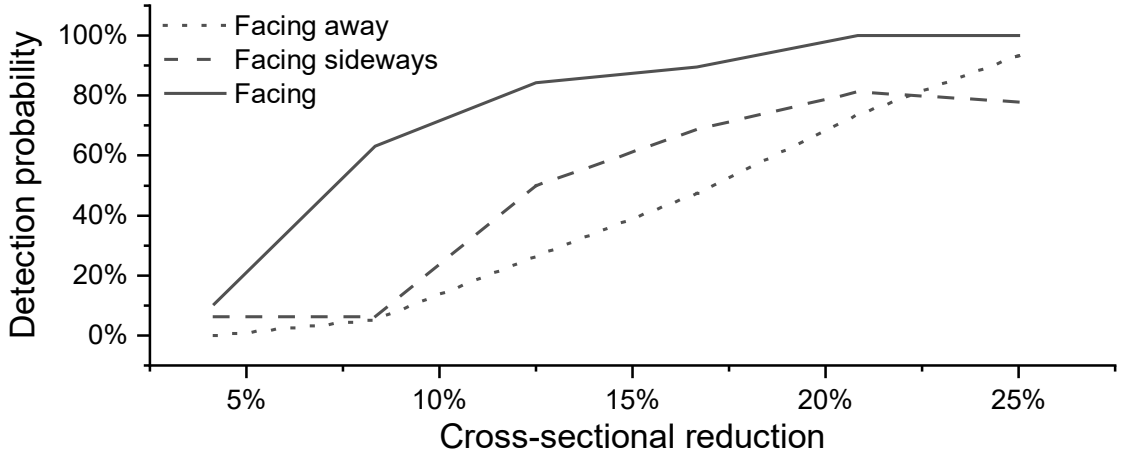

Fig. 9: Detection probability considering cross-sectional reduction and fracture orientation

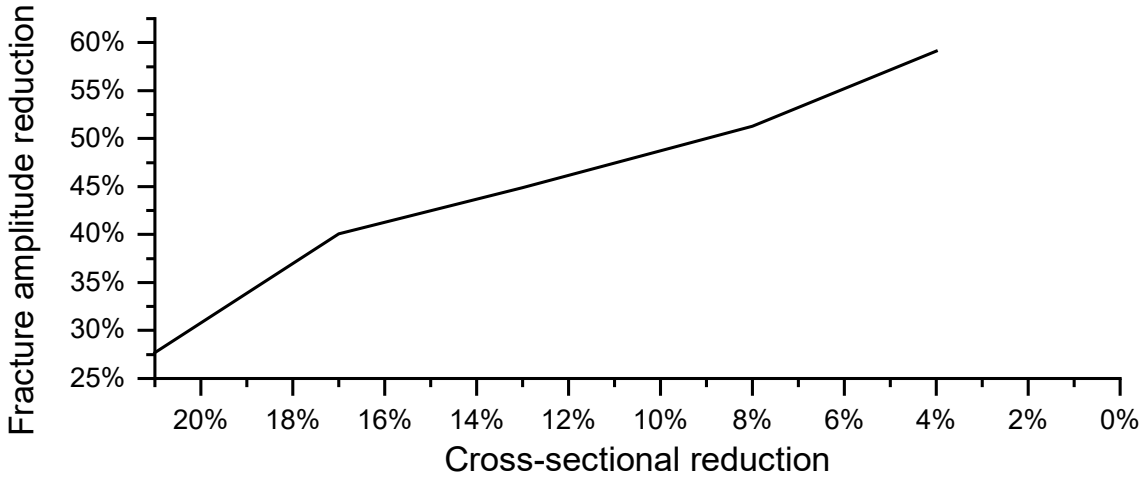

Fig. 10: Fracture amplitude reduction related to the fracture amplitude at 25 % cross-sectional reduction considering cross-sectional reduction

5.1.3 Position in relation to stirrups

The position in relation to the stirrups has a well quantifiable influence. Taking all data into account, the probability of detection above the stirrup is 64 % and between the stirrups 56 %. The detection probabilities differ only slightly for different cross-sectional reductions as well as in other subcategories.

It is similar for the fracture amplitude reductions. Looking at all values, the mean value of the fracture amplitudes above the stirrup is 1192 A/cm² and in between the stirrups 1176 A/cm², which corresponds to a reduction of 1 %. If the extent of the fracture amplitude reduction is taken into account, it can be said that the position in relation to the stirrups is not a decisive influencing factor. Presumably, this is because the filtering methods work.

5.1.4 Probe distance

The probe distance has an enormous influence on the detection probabilities. At a distance of 6.3 cm, 63 % of all fractures can be detected. If the distance is increased to 10.5 cm, only 37 % can be detected. Fig. 11 shows the detection probabilities considering cross-sectional reduction and probe distance. It must be pointed out at this point that the sample size for fractures with a probe distance of 10.5 cm is significantly smaller with 111 than that for 6.3 cm with 219. This means that statistical inaccuracies can occur more easily in this category. Nevertheless, the overall behaviour is good to see and is in line with the literature.

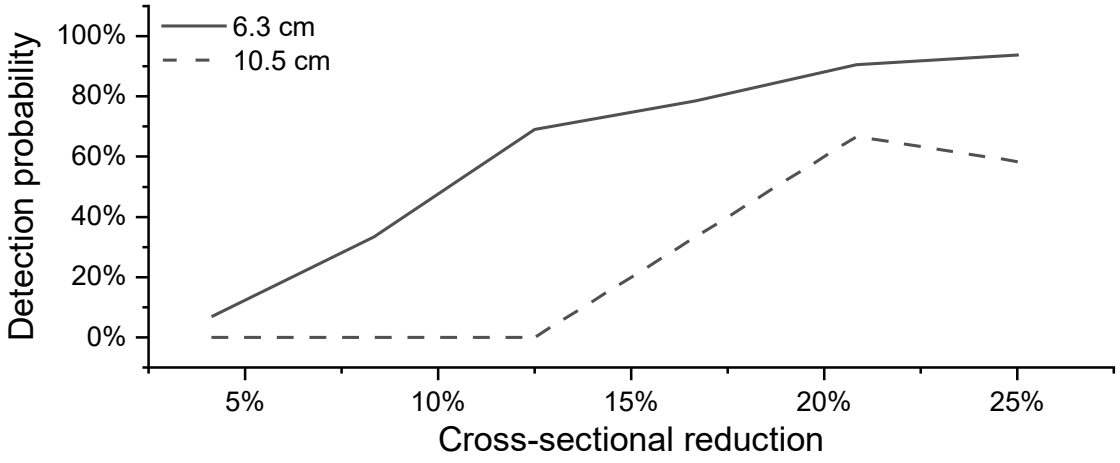

Fig. 11: Detection probability considering cross-sectional reduction and probe distance

The fracture amplitude reduction from 6.3 cm to 10.5 cm probe distance is relatively large. The fracture amplitude reduction is 45 % at 17 % cross-sectional reduction and 48 % at 21 % cross-sectional reduction when the distance is increased

from 6.3 cm to 10.5 cm. At 25 % cross-sectional reduction it is 42 %. With the same cross-sectional reduction, the fracture amplitude reduction is 11 % when the probe distance is increased from 4.0 cm to 6.3 cm and 48 % when the test head distance is increased to 10.5 cm.

The influencing factor of the probe distance is relatively complex, as it is influenced by various factors. On the one hand, the steel is weaker magnetised at a greater magnetic distance, and on the other hand, the magnetic field sensors are also further away from the magnetic field, which is why this signal becomes even weaker. The weaker signal also leads to lower fracture amplitudes and detection probabilities. As can be seen in Fig. 11, at a probe distance of 10.5 cm and a cross-sectional reduction of 21 %, 67 % of the fractures are detected and at 25 %, 62 % are detected. This is a cause for concern, as the previous method limits indicate a reliable detection of such cross-sectional reductions up to a depth of 20 cm. Assuming that the fracture is facing the probe which is likely due to the damage mechanism, a probe distance of 10.5 cm and cross-sectional reductions of 21 % and 25 % result in a detection probability of 100 %. Fractures facing away can be detected with a probability of 50 % for a cross-sectional reduction of 21 % and 43 % for a cross-sectional reduction of 21 %. This illustrates how the process limits can be pushed to their limits by unfavourable combinations of the influencing factors.

5.1.4 Combinations of the influencing factors

One of the most interesting ways to look at the data is to combine the influencing factors and push fracture detection to its limits. Fig. 12 illustrates what happens to the fracture amplitudes when the probe distance, fracture orientation and cross-sectional reduction are varied. For this purpose, the mean values of the fracture amplitudes in the respective category were plotted in the y-direction. The degree of cross-sectional reduction is given in the x-direction. At a probe distance of 6.3 cm and a facing fracture, clear and distinct fracture amplitudes can be seen. The fracture amplitude at a cross-sectional reduction of 25 % is 2297 A/cm². If the distance of the probe is increased to 10.5 cm or the fracture is rotated to facing away, the fracture amplitudes decrease significantly. If one of the two factors is varied, e.g. the fracture orientation is rotated from "facing" to "facing away" at a probe distance of 6.3 cm, a fracture amplitude reduction of about 66 % is obtained with a cross-sectional reduction of 25 %. Varying both parameters, increasing the probe distance to 10.5 cm and rotating the fracture from "facing" to "facing

away", results in a fracture amplitude of 609 A/cm² with the same cross-sectional reduction, which corresponds to a reduction of 73 %. In practice, such a combination of influencing factors can lead to significant cross-sectional reduction not being reliably detected.

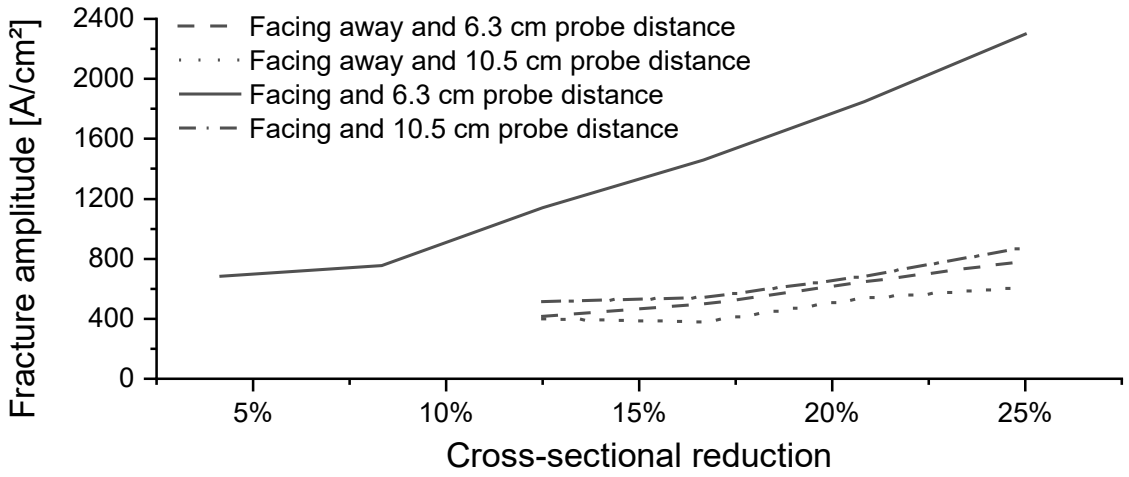

Fig. 12: Fracture amplitudes considering probe distance, fracture orientation and cross-sectional reduction

5.2 Magnetic interferences

The results of this test series can be summed up quite quickly: None of the installed rebar arrangements produced a fracture-like signal in the expected way. Rebars tested without any other interferences formed a magnetisation curve very similar to that of stirrups and were also recognised as stirrups by the filter algorithm. The set-up in the reinforcement cage and a prestressing steel strand with a cross-sectional reduction of 25 % showed that the various rebars had no quantifiable influence on the fracture amplitude.

The two set-ups with rebars in the reinforcement cage and subsequently with unbroken prestressing steel strands also provided unexpected data. One particular way of looking at the data was quite revealing. The results of the evaluation of all fracture amplitudes are entered in Fig. 13. A total of 374 fracture amplitudes were detected, which is on average 5 fracture amplitudes per measurement. Of these, 192 were with reinforcement cage only and 182 in the reinforcement cage with unbroken prestressing steel. To assist in the search for the cause, the stirrups with their corresponding stirrup number are drawn in Fig. 13 with vertical lines, where thin lines are normal stirrups with a diameter of d = 16 mm and thick lines are

overlapping open stirrup ends. The additional rebars whose position has been alternated between over the stirrup and in between stirrups are marked with an "S" above the vertical line.

It can be seen that the spatial rebars trigger a fracture amplitude, which, however, hardly stands out from the other fracture amplitudes. There are some conspicuous features when looking at the data. All fracture amplitudes form local groups that repeat themselves relatively regularly. These groups are all between the stirrups at about 100 cm, 130 cm, 160 cm, 190 cm and 220 cm. This is also exactly the stirrups spacing of 30 cm. The signals of the additional rebars between the stirrups form a small group at 150 cm and those above the stirrup fall into the group at 160 cm, again making it unclear how large the influence of the additional rebars is compared to the fracture amplitudes triggered by the reinforcement cage. The problem of fracture amplitudes triggered by regular reinforcement seems to be more decisive than the specifically installed additional rebars. Furthermore, it is noticeable that for the groups at 100 and 130 cm, the unbroken prestressing steel led to a significant increase in amplitude, which did not happen for the groups at 190 and 220 cm.

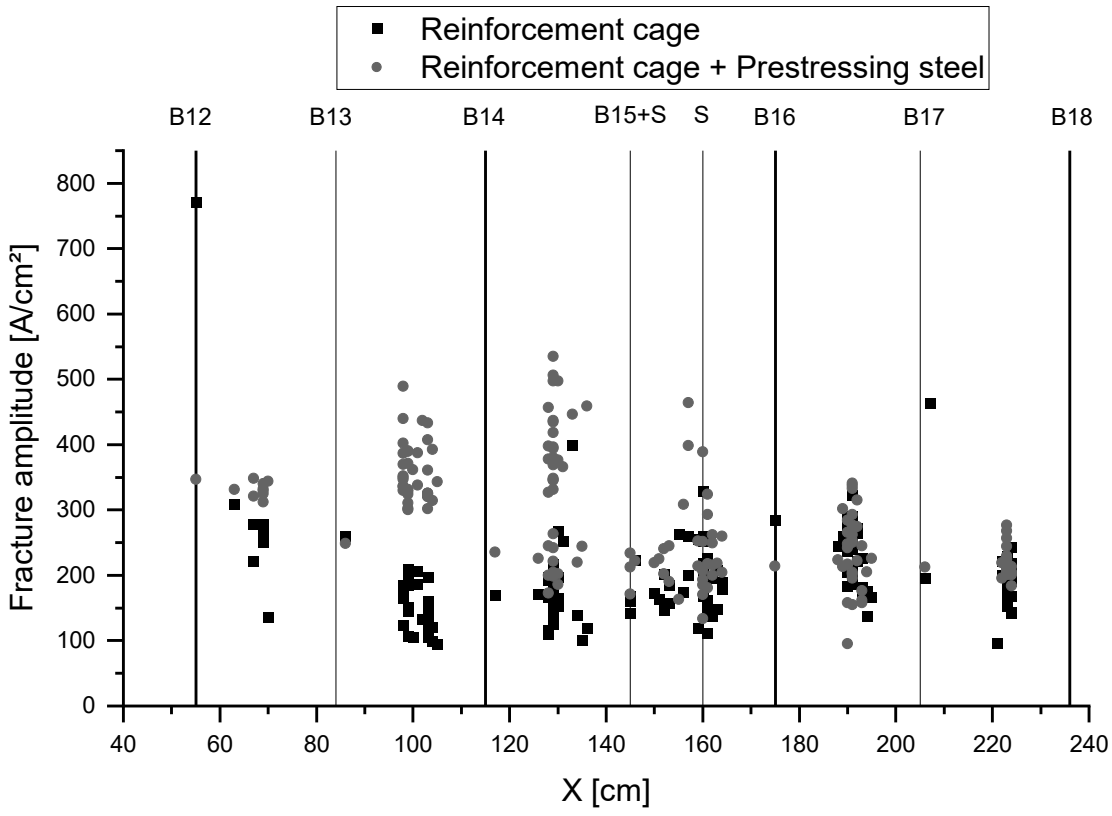

Fig. 13: Overview of all fracture amplitudes in the reinforcement cage with and without prestressing steel

To put the results presented into perspective it is important to look at the amplitude level. The average fracture amplitude of the empty reinforcement cage with additional rebars is 197 A/cm². Adding the unbroken prestressing steel increases the fracture amplitude to 285 A/cm². The highest fracture amplitude in Fig. 13 is 772 A/cm² at 55 cm, which is close to the non-inspectable end zone, where magnetic irregularities can occur and it can also be evaluated as a statistical outlier. The second highest fracture amplitude is 535 A/cm² at 126 cm. These fracture amplitudes can be compared to the ones shown in Fig. 12. Under favourable boundary conditions, 6.3 cm probe distance and a facing fracture, the false fracture amplitudes do not affect the fracture detection. At a cross-sectional reduction of 25 % it is 2297 A/cm² and clearly stands out next to the false fracture amplitudes. With a probe distance of 10.5 cm, a fracture facing away and a cross-sectional reduction of 25 % the average fracture amplitude is 609 A/cm². It is only slightly higher then the fracture amplitudes triggered by the reinforcement cage with unbroken prestressing steel. Fig. 12 shows that smaller cross-sectional reductions induce even smaller fracture amplitudes.

6. THRESHOLD VALUE

In the past, the false fracture amplitudes were filtered out by setting a threshold value of 700 A/cm². This characteristic value from practice coincides with the data shown in Fig. 13. In addition, it could be confirmed by the creation of a threshold diagram using data from test series 1 to 9. Here, the highest fracture amplitude from each set-up was determined and all values above a set threshold were counted. These were divided in ones that found the fracture and false fracture amplitudes, that didn’t find the installed fracture. In the last step, the distance between the two curves was determined. The maximum of the distance indicates the threshold at which the largest number of fractures was found correctly and at the same time the smallest number of false fracture amplitudes were present.

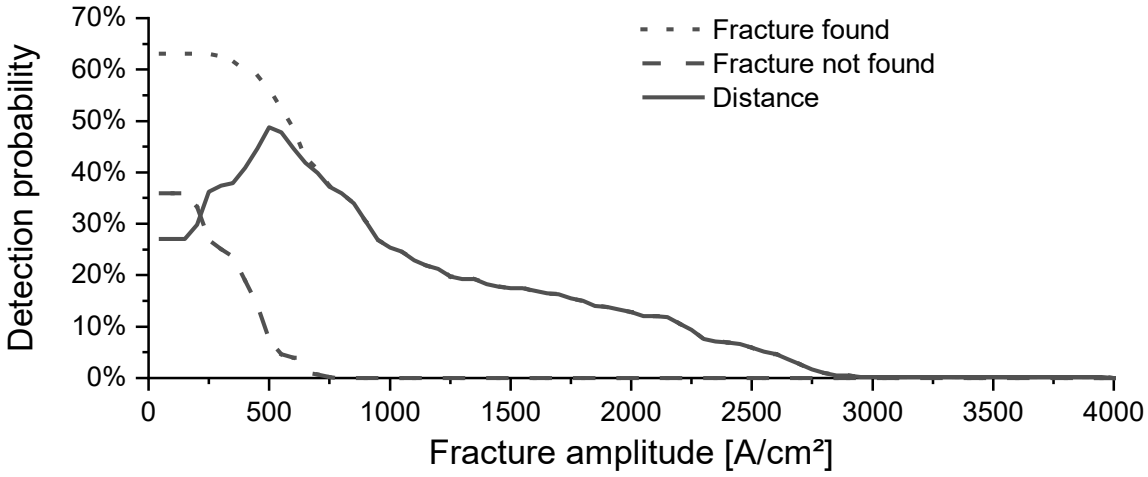

Fig. 14: Threshold diagram

Fig. 14 shows the created threshold diagram. If the threshold value is set to 0 A/cm², all values are above the threshold. Of these, 63 % are correct and 37 % are false fracture amplitudes. If the threshold is increased to 250 A/cm², 90 % of the values are higher. Of these, 63 % are correct and 27 % are false fracture amplitudes, which means that the distance between the two curves in the y-direction is 36 %. The greatest distance between the two curves is at 500 A/cm². Where, 64 % of the fracture amplitudes are still above the set threshold, whereby 56 % are correct and 7 % are false fracture amplitudes. It is particularly interesting that from a threshold value of 800 A/cm² no more false fracture amplitudes appear. This means that the set threshold value of 700 A/cm² can be confirmed and is a sensible measure. However, if the number of false fracture amplitudes would be reduced, the application limits could be expanded by reducing the threshold.

7. COMPARISON OF THE RESULTS WITH THE ESTABLISHED APPLICATION LIMITS

The established application limits make statements on concrete cover, degree of cross-sectional reduction and density of the reinforcement arrangement. The concrete cover and the degree of reduction of the cross-section have already been quantified by research work. Prestressing steel fractures are basically considered detectable up to a concrete cover of 20 cm. Fractures in prestressing steel strands are considered to be reliably detectable from a cross-sectional reduction of 20 %.

In the tests of this work, the fracture detection probability for fractures with more than 20 % cross-sectional reduction was 91 %. This accuracy was achieved even though not only facing fractures were included, but also fractures facing sideways

and facing away. Due to the damage mechanism, facing fractures are the most likely orientation in practice. Of these, 89 % of the fractures could still be detected at 17 % cross-sectional reduction. From 20 % cross-sectional reduction, it was even 100 %. In the case of the fractures facing away, 88 % of the fractures with a cross-sectional reduction of more than 20 % could be detected.

Since only one variant of the reinforcement arrangement was investigated, no statements can be made about the influence of the density of the reinforcement. However, it is obvious that the filter methods work, as all of the above fracture detection probabilities were obtained with the interference of the reinforcement cage. The effectiveness of the filtering methods is particularly evident when considering the small influence of position in relation to stirrups on fracture detection and fracture amplitudes. Furthermore, it was shown that most irregular reinforcement arrangements are detected by the filter methods and have no influence on the fracture detection. The influencing factor of the probe spacing has to be evaluated more critically, but the available data are not sufficient to restrict the previous application limit of 20 cm detection depth. At the largest investigated probe spacing of 10.5 cm, 100 % of the facing fractures and 46 % of the fractures facing away could still be found at a cross-sectional reduction of 20 % or more. Further research on the influence of the probe distance would be recommended. Even more important than the evaluation of the influence, however, would be the development of methods to minimise the negative influence of large probe distance, to extend the procedural limits and to increase the safety of the examined structures.

8. EXPANDING APPLICATION LIMITS AND DEVELOPMENT OPPORTUNITIES

The magnetic flux leakage test was able to achieve good results within the established application limits. However, it could be shown through a systematic variation and combination of the influencing factors that fractures of cross-sectional reductions above 20 % can produce small fracture amplitudes under unfavourable conditions. Here, the probe distance and thus the concrete cover play a particularly decisive role. This dominant role of the probe distance is already known from previous research. When evaluating these results, it was assumed that even low fracture amplitudes can still be assessed. However, this is only true under the condition that there are relatively few false fracture amplitudes. If the results on the

influence of the magnetic interferences are included in the consideration, it becomes apparent that, apart from the many small false fracture amplitudes, only large and unambiguous ones can be detected. This means that the established application limits and the set threshold are not always on the safe side.

An improvement of the detection probabilities can be achieved by two directions of development:

1. increase of the detection capacity
2. reduction of the threshold.

Both options can be achieved mainly at the level of the evaluation algorithms. One of the few physical measures that could lead to an increase in detection capacities is an increase in magnetisation. It could be tested whether an increase in magnetisation can be achieved by stronger magnets, more frequent passes or remaining field measurements after stronger magnetisation steps. However, the experiments on the influence of the magnetic interferences suggest that in this case the false fracture amplitudes could also increase.

A reduction of the threshold value is equivalent to a reduction of the false fracture amplitudes. Here, the multi-step filtering methods must be considered in more detail. One significant filtering method is remaining field summation, which eliminates many stirrup signals. A weakness of the existing protocol is that it is not known how exactly the coercive magnetic field strength of the reinforcing steel was achieved when the stirrup magnetisation was reversed. Furthermore, it is noticeable in many experiments that remaining field measurement 1 and 2 show deviating shapes, which prevents an elimination of the signals. One possibility for improvement could be to carry out further runs for demagnetisation after the reversal of the stirrup magnetisation. The aim of these further runs is to completely demagnetise the stirrups. For this purpose, the magnetic flux leakage system automatically reads the stirrup magnetisation at the stirrup locations and alternates the pole strength until a fixed limit value of the stirrup magnetisation is reached. Tests on the magnetic material behaviour have shown that the longitudinal bars are not demagnetised by this, but that the magnetisation still increases, the prestressing steel with its potential fracture amplitudes should become more apparent as a result.

The evaluation of the magnetic interferences in the reinforcement cage, carried out with and without unbroken prestressing steel, shows that it is not only due to

specific metallic interferences that the false fracture amplitudes occur. It must be a combination of the influences of the reinforcement cage and the evaluation algorithm. This is especially good news because the evaluation algorithms are within our own control and can be improved. The regularity along the x-axis and the large influence of the unbroken prestressing steel are both indications that the occurrence of the false fracture amplitudes is systematic in nature. This also suggests that by improving the filtering algorithm, the false fracture amplitudes can be significantly reduced.

To improve fracture detection, one could test the effectiveness of different fracture signals that deviate from the previous idealised fracture signal. This is a particularly easy place to test changes because different signals can be used in parallel. In this way, the magnetic flux leakage test system can still be used classically in the industrial orders and new evaluation possibilities can be researched at the same time.

If the idea of using different fracture signals in parallel is developed, it is also possible to imagine that the correlation analysis is not only carried out at the end of the entire filter process. It could also be tested at different intermediate stages. At this point, the fracture shapes will still deviate from the idealised fracture signal, which is why fracture signals should be used that originate from exactly this stage of the filtering process. For this purpose, measurement signals from laboratory tests can be used in which a good correlation was present in the last step.

Since the break signals from the intermediate stages are less changed by the filter methods, they are more strongly shaped by the influencing factors. So, there is the possibility that fracture signals have a specific fracture shape depending on which boundary conditions are present. The correlation analysis accesses not only one fracture signal in all intermediate stages and after the complete filter process, but a database that contains fracture signals under different boundary conditions. In this way, fractures could be detected whose signal was changed too much by the boundary conditions to correlate with the idealised fracture signal. Depending on which non-ideal fracture signals, modified by the boundary conditions, the measured signal correlates with, one can perhaps also draw conclusions about the boundary conditions.

Since every change to the magnetic flux leakage test system must first be verified by trials, the development cycles for implementation can be very long. However, for testing changes to the evaluation algorithms, it is not necessary to repeat all

laboratory tests each time. The raw data of the test series can be reused and re-evaluated. The raw data of the measurement curves could be stored in a database to which the evaluation algorithm to be tested has access. In this way, it can access all existing raw data one after the other, evaluate them and then present the results. In this way, many of the statistics and diagrams that were created manually for this Master's thesis could be created automatically by a script in the future. Based on the statistics, one can thus get an overview of how effective the change was for fracture detection.

Having discussed the potential development of magnetic flux leakage measurement, it is necessary to remember that there are no alternative methods that can detect prestressing steel fractures in a comparable way. At the same time, the bridge stock of Germany and Europe continues to age. A large number of bridge and building structures were built in the 1950s to 1970s using prestressed concrete construction methods, in some cases using tempered prestressing steels in which sudden failure can occur. If the accuracy and fracture detection of magnetic flux leakage test are improved, the safety of the structures and thus traffic safety can be increased enormously [1, 12].

REFERENCES

[1] LEHMANN, F.: *MPA Universität Stuttgart, Dienstleistung Magnetische Streufeldmessung,* Materialprüfungsanstalt Universität Stuttgart, [Online]. Available: https://www.mpa.uni-stuttgart.de/ingenieur_und_pruef-dienstleistungen/Detailseiten/magnetische-streufeldmessung/. [Zugriff am 15 August 2022]

[2] DOBRINSKI, P.: *Physik für Ingenieure* Viewg+Teubner, Wiesbaden, 2010

[3] WIKIMEDIA FOUNDATION INC: Wikipedia – Die freie Enzyklopädie, Wikimedia Foundation Inc, 2 August 2022. [Online]. Available: https://de.wikipedia.org/wiki/Ferromagnetismus. [Zugriff am 18 August 2022]

[4] STEINFELD, B.: *Untersuchungen zur Bestimmung der Nachweisgrenzen der Detektion von Spannstahlbrüchen in Spannbündeln mit der Methode der magnetischen Streufeldmessung,* Materialprüfungsanstalt Universität Stuttgart, Stuttgart, 2014

[5] SAWADE, G.: *Prüfung von Spannbetonbauteilen mit magnetischen Methoden* Beton- und Stahlbetonbau 105, Heft 3, pp. 154-164, 2010

[6] HILLEMEIER, B.: *Die Überprüfung von Spannbetonkonstruktionen auf Unversehrtheit der Spannglieder,* Bautechnik, November 2011

[7] TAFFE, A.: *Zerstörungsfreie Zustandsermittlung und Qualitätssicherung in der Betoninstandsetzung,* Beton- und Stahlbetonbau Spezial, pp. 1-13, Dezember 2008

[8] WALTHER, A.: *Vergleichende Signalinterpretation von Spannstahlbrüchen im remanenten und aktiven magnetischen Streufeld, Dissertation* Technische Universität Berlin, Berlin, 2012

[9] SCHEEL, H.: *Ortung von Spannstahlbrüchen in metallischen Hüllrohren, Abschlußbericht zum Forschungsauftrag des Deutschen Instituts für Bautechnik AZ: IV 1-5-672/92* Deutsches Institut für Bautechnik AZ, Berlin, 1996

[10] DGZfP Fachausschuss für Zerstörungsfreie Prüfung im Bauwesen Unterausschuss Magnetische Verfahren zur Spannstahlbruchortung: *Positionspapier Magnetische Verfahren zur Spannstahlbruchortung* DGZfP Fachausschuss für Zerstörungsfreie Prüfung im Bauwesen, Berlin, 2017

[11] MIKERUN: *Growing-magnetic-domains* Wikimedia Commons, 2 August 2020. [Online]. Available: https://commons.wikimedia.org/wiki/File:Growing-magnetic-domains.svg. [Zugriff am 18 August 2022]

[12] BUNDESMINISTERIUM FÜR VERKEHR, BAU UND STADTENTWICKLUNG ABTEILUNG STRAßENBAU: *Handlungsanweisung Spannungsrisskorrosion* Bundesanstalt für Straßenwesen, 2011